Materials Science Forum
ISSN: 1662-9752, Vol. 1062, pp 371-375
doi:10.4028/p-ryui6b

Submitted: 2021-10-25
Revised: 2022-02-16
Accepted: 2022-03-17
Online: 2022-05-31

Stability, Evolution and Diffusion of Intrinsic Point Defects in 4H-SiC

Marianne Etzelmüller Bathen[1,a*], Robert Karsthof[2,b], Ulrike Grossner[1,c] and Lasse Vines[2,d]

[1]Advanced Power Semiconductor Laboratory, ETH Zürich, 8092 Zürich, Switzerland

[2]Department of Physics, University of Oslo, N-0316 Oslo, Norway

[a*]bathen@aps.ee.ethz.ch, [b]r.m.karsthof@fys.uio.no, [c]ulrike.grossner@ethz.ch, [d]lasse.vines@fys.uio.no

*Corresponding author

Keywords: Point defects, deep level transient spectroscopy, silicon carbide, carbon interstitial, carbon antisite-vacancy pair

Abstract. Silicon carbide (SiC) is a wide band-gap semiconductor of great technological importance, showing promise for application areas ranging from quantum computing and communication to power devices. Vital in both the contexts of power devices and quantum technology is the understanding of intrinsic defects that are introduced during various device processing steps, both immediately after their formation and over the course of defect evolution with temperature. Here we monitor the formation and evolution of intrinsic point defects in n-type 4H-SiC after proton irradiation at room temperature and subsequent annealing in the temperature range 300 – 1000 °C, and discuss the nature and origin of the EH_4 and EH_5 deep level defects observed by deep level transient spectroscopy around 400 – 500 K. In particular, the controversy on the nature of the EH_5 trap in particular is addressed, where we propose the presence of two overlapping defect peaks: one metastable level that appears after low energy electron irradiation below the silicon displacement limit, and one more stable level that gradually decreases in concentration until an annealing temperature of 1000 °C. We argue that the former is likely related to carbon interstitials, while the latter was recently tentatively attributed to the carbon antisite-vacancy pair.

Introduction

The carbon and silicon vacancies in 4H-SiC (V_C and V_{Si}, respectively) have been studied intensively [1] on account of (i) their detrimental impact on minority carrier lifetime and hence device performance, particularly in the case of V_C [2], and (ii) room temperature (RT) single-photon emission and spin manipulation for V_{Si} [3]. The latter characteristics, that are paramount for many quantum technology applications, have also been demonstrated for complexes of the fundamental vacancies including the divacancy ($V_{Si}V_C$), the carbon antisite-vacancy pair ($C_{Si}V_C$) and the nitrogen-vacancy complex (N_CV_{Si}) [4].

The carbon antisite-vacancy (CAV) pair was predicted to be electrically active by density functional theory (DFT) calculations and having two sets of charge state transitions in the upper half of the band gap: (0/-) at around E_C – 0.5 eV and (+/0) at around E_C – 1.0 eV [5], with E_C denoting the conduction band edge. Recently, the (+/0) charge transition level (CTL) of the CAV pair was suggested to be responsible for the EH_4 and EH_5 levels often observed in deep level transient spectroscopy (DLTS) measurements of 4H-SiC [6]. The splitting between the EH_4 and EH_5 peaks of about 0.1 eV was also predicted theoretically [5] and can be explained by a difference in CTL energy for the four different CAV configurations (*hh*, *kk*, *hk* and *kh*) caused by the inequivalent hexagonal and pseudo-cubic lattice sites in 4H-SiC. Another recent work [7] employed photo-induced current transient spectroscopy (PICTS) and detected a level that was also assigned to the (+/0) transition of the CAV complex, but due to the use of high purity semi insulating (HPSI) samples with Fermi levels near mid gap, different annealing behavior would be expected as compared to the n-type samples used in Ref. [6]. Nonetheless, an important controversy remains. In Ref. [6], the EH_4 and EH_5 trap

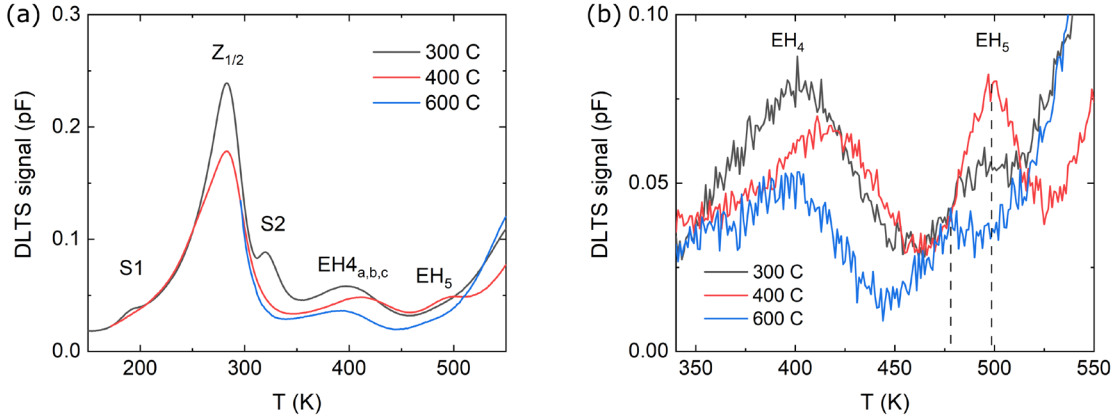

Fig. 1: DLTS spectra after 1.8 MeV proton irradiation to a fluence of 1×10^{12} cm^{-2} and a 300 °C post-anneal (black curves), followed by anneals at 400 °C (red) and 600 °C (blue). In (a) a standard lock-in weighting function and a 640 ms rate window were employed while (b) shows the corresponding high-resolution GS4 spectrum.

concentrations were reported to decrease steadily upon annealing at temperatures up to 1000 °C. Previous works [8] have reported the presence of EH_5 in samples irradiated with electrons at low energies below the silicon displacement limit, and a lower annealing temperature than expected for a complex defect like the CAV pair, drawing the assignment of EH_5 to the CAV pair into question.

In this contribution, we monitor the development of the resulting defect distribution after formation by proton irradiation and annealing up to 1000 °C. We pay particular attention to the EH_4 and EH_5 DLTS peaks that are often observed after irradiation of 4H-SiC and discuss the possibility of more than one defect species being involved in their appearance. The metastability of the EH_5 peak will also be discussed in this context.

Experimental Methods

We introduce intrinsic defects in 10 µm thick n-type (N doped) 4H-SiC epitaxial layers ($N_D \sim 1\times10^{15}$ cm^{-3}) using 1.8 MeV proton irradiation to a fluence of 1×10^{12} cm^{-2}. The substrates were n-doped to approximately 8×10^{18} cm^{-3}. All implantations were performed at room temperature and at an angle 8° off with respect to the surface normal to avoid channeling effects. The implantation peak was situated at around 27 µm leaving the defect distributions approximately uniform in the near-surface region. The evolution of the resulting defect distributions is monitored after several annealing steps at 300 –1000 °C. The heat treatments were performed in a conventional tube furnace for 30 min in N_2 flow. Schottky barrier diodes (SBDs) were formed by depositing 150 nm thick circular contacts (1 mm diameter) of Ni by evaporation through a shadow mask.

The defect signatures were detected using deep level transient spectroscopy (DLTS). DLTS measurements were carried out for temperatures in the range 150 – 650 K using a measurement frequency of 1 MHz, 20 ms pulse length and 10 V pulse height at a reverse bias of −10 V. Six rate windows between 20 and 640 ms were chosen for evaluation of the transients, using both standard lock-in and GS4 correlation functions. The concentrations of the defect levels observed in the spectra were extracted using numerical simulation of the DLTS spectra based on assumed variable values for trap energy, density and capture cross-section. The λ correction was taken into account.

Results and Discussion

The prevalent defects, measured by DLTS immediately after irradiation and a 300 °C post-anneal to alleviate some of the implantation damage, are as shown in Fig. 1(a). In the figure the S1 and S2 (S-center), $Z_{1/2}$, EH_4 and EH_5 levels can be clearly observed (along with the shoulder of $EH_{6/7}$). The S-center and $Z_{1/2}$ (and $EH_{6/7}$) levels have previously been assigned to the V_{Si} [9] and V_C [10] defects,

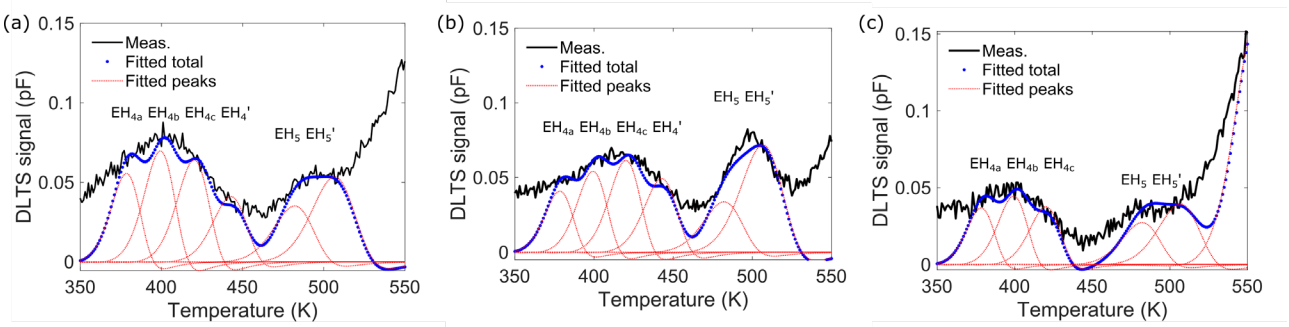

Fig. 2: DLTS spectra after 1.8 MeV proton irradiation to a fluence of 1×10^{12} cm^{-2} and post-anneals at (a) 300 °C, (b) 400 °C and (c) 600 °C. A high-resolution GS4 weighting function was employed (black solid curves) while the blue dotted curves show the cumulative sum of numerical simulations that are fitted to the spectra. Red dotted curves represent the individual fitted peaks.

respectively, while the EH_4 and EH_5 levels were tentatively assigned to the (+/0) charge state transition levels of the $C_{Si}V_C$ in four different configurations [6]. Further heat treatments at 400 and 600 °C see the reduction in S1, $Z_{1/2}$ and S2, likely caused by recombination with remaining Si and C self-interstitials that survived the initial 300 °C post-anneal [6].

Whereas the other peaks appear to diminish gradually as the temperature is increased, EH_5 exhibits discordant behavior. The EH_5 level is enhanced upon annealing at 400 °C before diminishing again for the 600 °C anneal. Taking a closer look, we find that the peak position appears to shift. Similar behavior is observed for EH_4 while the $Z_{1/2}$ peak remains immobile (see Fig. 1a), discounting a measurement artefact as being responsible for the shift.

Fig. 1(b) shows a high-resolution DLTS spectrum (using the GS4 weighting function) centered on the EH_4 and EH_5 peaks. Here, we can see the contours of two different peaks contributing to the EH_5 defect level. It seems that annealing at 400 °C promotes the growth of a portion of the EH_5 peak that quickly vanishes again after 600 °C annealing, while another part remains. We attribute this behavior to the presence of two different defect species giving rise to two peak components: the original EH_5 level, and a metastable one appearing at a higher (~20 K) temperature than EH_5 in the DLTS spectra and disappearing after higher temperature annealing.

Next, we perform numerical simulation of the DLTS spectra to fit the curves and extract parameters for the different features based on assumed variable values for trap energy, density and capture cross-section. The starting point for the simulations was the parameters for EH_4 and EH_5 presented in Ref. [11]. Importantly, both EH_4 and EH_5 appear to contain more features than previously expected. Fig. 2 shows experimental data (black curves), cumulative fits of the numerical simulations (blue dotted curves) and individual peak fits (red dotted curves) for high-resolution DLTS spectra (GS4 weighting function) of a proton irradiated sample annealed at (a) 300 °C, (b) 400 °C and (c) 600 °C. The fitting parameters employed are presented in Table 1.

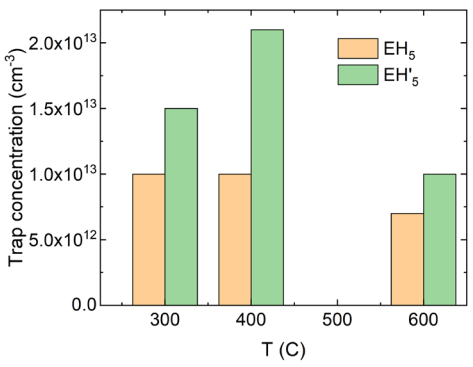

Fig. 3: Trap concentrations for EH_5 and EH'_5 extracted from numerical simulations of the DLTS spectra in Fig. 2.

As previously found [6], EH_4 contains at least three contributions a, b and c. However, we also observe the likely appearance of a fourth contribution (EH_4') after the 400 °C anneal, which rapidly disappears again above 600 °C. More contributions are possible, but further investigations are needed to deduce the complex fine structure of the EH_4 peak and its thermal evolution. Importantly, at least two contributions are also needed to fit the EH_5 peak: EH_5 (stable) and EH'_5 (metastable). The variables used for simulating the DLTS spectra are E_A=1.10 eV below E_C and $\sigma_n = 8\times10^{-15}$ cm^{-2} for EH_5, and $E_A=E_C$ –1.13 eV and $\sigma_n = 4.5\times10^{-15}$ cm^{-2} for EH'_5, σ_n denoting the electron capture cross section.

Table 1: Fitting parameters for the six observed trap levels, including the trap energy level below the conduction band edge (E_T), electron capture cross-section (σ_n) and trap concentration (N_T).

Trap name	E_T *(eV)*	σ_n *(cm²)*	N_T *(cm⁻³), 300 °C*	N_T *(cm⁻³), 400 °C*	N_T *(cm⁻³), 600 °C*
EH_4^a	0.93	1.0×10^{-13}	1.7×10^{13}	1.3×10^{13}	1.0×10^{13}
EH_4^b	0.985	1.0×10^{-13}	2.1×10^{13}	1.7×10^{13}	1.2×10^{13}
EH_4^c	1.04	1.0×10^{-13}	2.1×10^{13}	1.9×10^{13}	1.0×10^{13}
EH_4'	1.10	1.0×10^{-13}	1.2×10^{13}	1.5×10^{13}	0
EH_5	1.10	8.0×10^{-15}	1.0×10^{13}	1.0×10^{13}	7.0×10^{12}
EH_5'	1.13	4.5×10^{-15}	1.5×10^{13}	2.1×10^{13}	1.0×10^{13}

An important feature of the spectra in Fig. 2 is the thermal evolution of the different components of the EH5 peak. After the 300 °C heat treatments, the two contributions to the EH_5 peak are present in approximately similar amounts. Annealing at 400 °C leaves the more stable component of EH_5 constant or promotes a slight reduction while the metastable EH'_5 peak grows by ~40 %. At 600 °C and above, the EH_5' is reduced to about 50 % of its 400 °C value whereas the main EH_5 component exhibits a small decrease. While EH_5' disappears rapidly above 600 °C the more stable EH_5 is steadily reduced in concentration towards 1000 °C (not shown, see Ref. [6]). The dependencies of trap concentration on annealing temperature are visualized in Fig. 3.

The apparent presence of two distinct defect levels in the vicinity of EH_5 sheds light on an important discussion. The EH_5 peak has previously been observed in samples that were electron irradiated to low energies ≤ 200 keV, i.e., below the Si displacement limit [8]. Thus, its relation to the CAV pair has been questioned. Instead, we find that EH_5 has two components of different thermal stabilities, EH'_5 and EH_5. Such a possibility was suggested, but not demonstrated, in Ref. [10]. One component of EH_5, termed EH'_5 herein, is assumed to be responsible for the metastability observed in Ref. [8], coming up when we anneal the irradiated sample at 400 °C but quickly dies afterwards. The other part is the actual EH5, which is more stable and decreases slightly with annealing temperature up to 1000 °C [6]. Previous works [8,11] have reported on this metastability but not separated the two different contributions from one another.

Finally, we speculate that the metastable peak near EH_5, EH'_5, is likely related to C interstitials as it appears after 200 keV electron irradiation when, e.g., the S-center is not present. The actual EH_5 peak, however, is correlated to the occurrence of S1, S2 and EH_4 and persists at substantially higher temperatures. Thus, we reinforce the previous assignment of EH_5 to the (+/0) charge-state transition of the CAV pair while the metastable behavior is tentatively attributed to carbon interstitial related defects.

Concluding Remarks

We study proton irradiated n-type 4H-SiC epitaxial layers after annealing at different temperatures and monitor the evolution of the defect population. The traps commonly named EH_4 and EH_5 are studied, and their properties extracted by fitting to numerical simulation of DLTS spectra. We reinforce that the EH_4 level contains at least three contributions, previously assigned to the (+/0) CTL of the CAV complex, with the potential addition of neighboring levels that respond differently to annealing than the other components. In the case of EH_5, two defect levels are needed to explain the DLTS signal. The main contribution to EH_5 appears after irradiation and decreases slowly in concentration up to 1000 °C. The second EH_5 component, labeled EH'_5 herein, grows substantially upon 400 °C annealing and disappears rapidly afterwards. In short, we propose that the EH_5 trap in fact embodies two different defect levels: one that is metastable and related to carbon interstitial defects, whereas the other is more stable persisting until 1000 °C and is tentatively assigned to the (+/0) CTL of the carbon antisite-vacancy pair.

References

[1] N. Iwamoto and B. Svensson, in Defects in Semiconductors, vol. **91** of Semiconductors and Semimetals, edited by L. Romano, V. Privitera and C. Jagadish (Elsevier, 2015) p. 369.

[2] K. Danno, D. Nakamura and T. Kimoto, Applied Physics Letters **90**, 202109 (2007).

[3] M. Widmann, S.-Y. Lee, T. Rendler, et al., Nature Materials **14**, p. 164-168 (2015).

[4] G. Zhang, Y. Cheng, J.-P. Chou and A. Gali, Applied Physics Reviews **7**, 031308 (2020).

[5] K. Szász, V. Ivády, et al., Phys. Rev. B **91**, 121201(R) (2015).

[6] R. Karsthof, M. E. Bathen, A. Galeckas and L. Vines, Physical Review B **102**, 184111 (2020).

[7] H. Nakane, et al., J. Appl. Phys. **130**, 065703 (2021).

[8] F. C. Beyer, et al., J. Phys. D: Appl. Phys. **45**, 455301 (2012).

[9] M. E. Bathen, A. Galeckas, et al., npj Quantum Information **5**, 111 (2019).

[10] N. T. Son, X. T. Trinh, et al., Physical Review Letters **109**, 187603 (2012).

[11] G. Alfieri, et al., J. Appl. Phys. **98**, 043518 (2005).